

The Effects of the Inertial Properties of Above-Knee Prostheses on Optimal Stiffness, Damping, and Engagement Parameters of Passive Prosthetic Knees

Yashraj S. Narang

School of Engineering and Applied Sciences

Harvard University

Cambridge, Massachusetts 02138

email: ynarang@seas.harvard.edu

V. N. Murthy Arelekatti

Department of Mechanical Engineering

Massachusetts Institute of Technology

Cambridge, Massachusetts 02139

email: murthya@mit.edu

Amos G. Winter, V

Assistant Professor

Department of Mechanical Engineering

Massachusetts Institute of Technology

Cambridge, Massachusetts 02139

ASME Member

email: awinter@mit.edu

ABSTRACT

Our research aims to design low-cost, high-performance, passive prosthetic knees for developing countries. In this study, we determine optimal stiffness, damping, and engagement parameters for a low-cost, passive prosthetic knee that consists of simple mechanical elements and may enable users to walk with the normative kinematics of able-bodied humans. Knee joint power was analyzed to divide gait into energy-based phases and select mechanical components for each phase. The behavior of each component was described with a polynomial function, and the coefficients and polynomial order of each function were optimized to reproduce the knee moments required for normative kinematics of able-bodied humans. Sensitivity of coefficients to prosthesis mass was also investigated. The knee moments required for prosthesis users to walk with able-bodied normative kinematics were accurately reproduced with a mechanical system consisting of a linear spring, two constant-friction dampers, and three clutches ($R^2 = 0.90$ for a typical prosthetic leg). Alterations in upper leg, lower leg, and foot mass had a large influence on optimal coefficients, changing damping coefficients by up to 180%. Critical results are reported through parametric illustrations that can be used by designers of prostheses to select optimal components for a prosthetic knee based on the inertial properties of the amputee and his or her prosthetic leg.

Keywords: Prosthetic Knee, Component Optimization, Prosthesis Mass, Design for the Developing World, India

1 Introduction

Our research aims to design low-cost, high-performance prosthetic knees for above-knee amputees in developing countries. Specifically, our goal is to design a fully passive prosthetic knee mechanism for users in India, which can facilitate able-bodied gait kinematics and cost less than \$100 to fabricate. According to the World Health Organization, approximately 30 million people worldwide are in need of prosthetic and orthotic devices [1–3]. There are approximately 230,000 above-knee amputees in India [4,5], the country where our research is currently focused. Since many of these individuals experience poverty [6], unemployment, and social discrimination [3] due to their disability, they have a major need for a low-cost prosthetic knee that allows them to walk with able-bodied gait patterns, be employed, and appear able-bodied. However, low-cost prosthetic knees available in developing countries are typically locked knees, single-axis knees with constant-friction resistive elements, and four-bar knees with constant-friction resistive elements [3,7,8], all of which may significantly inhibit users from walking with the gait patterns similar to that of able-bodied humans [9]. This paper presents biomechanical analysis and theoretical optimization aimed at designing a low-cost prosthetic knee that could closely replicate the able-bodied knee moment and thereby effectively facilitate able-bodied gait kinematics of lower limbs. We use the terms “able-bodied kinematics” and “normative gait kinematics” to refer to the normative lower limb gait kinematics collected from a population of able-bodied humans.

A major goal of prosthetic knees is to enable above-knee amputees to walk with normative gait kinematics. When an able-bodied human walks, the muscles, tendons, and ligaments adjacent to the knee produce moments that flex and extend the knee to enable kinematics that are necessary for walking with high metabolic efficiency [10]. However, for an above-knee amputee, musculotendon function is impaired. Designers of prosthetic knees have attempted to provide the musculotendon

function required for normative kinematics using active electromechanical systems [11, 12]. Many of these devices are designed to avoid kinematic gait deviations in above-knee amputees, such as abduction, circumduction, vaulting, uneven heel rise, stumbles, and falls [13, 14]. However, due to the high initial and maintenance costs of such systems, prosthetic knees for developing countries typically consist of passive mechanical elements that do not change during gait [15, 16]. Thus, in designing prosthetic knees for the developing world, as well as other passive knees, it is critical to characterize and quantify the biomechanical function of the knee required for normative gait kinematics and select components to accurately reproduce the desired motion. In this context, the term “biomechanical function” of the knee refers to the moment-angle and moment-time relationships of the knee joint, and their effect on lower limb gait dynamics, as described in the following paragraphs.

Researchers have used multiple methods to quantify the biomechanical function required for normative walking on flat ground. Several studies have examined specific regions of the gait cycle and calculated the derivative of the moment-angle relationship of the able-bodied knee during walking. These studies have demonstrated that the moment-angle relationship has a nearly constant derivative during parts of the gait cycle (e.g., weight acceptance) and that the phenomenon is consistent for multiple walking speeds and load carriage conditions [17–19]. For prosthesis design, these results imply that a prosthetic knee could partially replicate the biomechanical function of an able-bodied knee during walking using torsional springs with a linear force-displacement relationship.

Other studies have quantified the knee’s biomechanical function by designing a mechanical model, describing each component with a polynomial function, and optimizing the coefficients (referred to here as Mechanical Model Coefficients, or MMC) to closely reproduce the moment-time relationship of the able-bodied knee during normative walking [11, 12]. These studies have divided gait into specific phases, modeled the knee with components of varying polynomial order during each phase (e.g., linear spring, nonlinear damper), and optimized the coefficients of the components to reproduce the moment-time relationship. In the context of prosthesis design, each of the studies determined a configuration of components that allowed a prosthetic knee to accurately replicate the biomechanical function of an able-bodied knee during walking.

The previous studies discussed above [3, 11–13, 16] have two significant limitations with respect to their implications for prosthesis design. First, the studies quantified the biomechanical function based on a leg with able-bodied inertial properties moving with normative kinematics. Since the masses of prosthetic leg segments are typically lower than those of able-bodied segments [20], the knee moment required to produce normative kinematics is different [21]. Second, the studies determining MMC did not report the sensitivity of the moment-time relationship of the model to the complexity of the components. It is possible that a simple configuration of components with a constant or linear force-displacement relationship can accurately reproduce the moment-time relationship for walking, which would facilitate the design of low-cost, high-performance prosthetic knees.

The goal of the present study was to determine optimal stiffness, damping, and engagement parameters for a passive prosthetic knee by designing a mechanical model of the knee and determining MMC. In contrast to previous studies, MMC were optimized to allow the model to accurately reproduce the moment-time relationship required for a lightweight prosthetic leg to move with normative kinematics, as opposed to the moment-time relationship required for an able-bodied leg to do

so. In addition, the sensitivity of the accuracy of the model to the polynomial order of components was investigated, and the effects of inertial properties of the prosthetic leg on MMC were determined. Results are reported in the form of parametric illustrations that can be readily used by researchers, designers, and prosthetists. Our methods and outcomes have the potential to improve the design of low-cost, high-performance prosthetic knees for the developing world, as well as prosthetic knees in general.

2 Methods

2.1 Gross effects of inertial properties on the required knee moment required for achieving normative kinematics

To determine the knee moment (T_{req}) required to produce normative kinematics at a natural walking cadence (105 steps/min) [22] for various inertial configurations of a prosthetic leg, a rigid body model of the prosthetic leg was designed and inverse dynamics was performed according to the methods presented in Narang et al. [21]. Narang et al. used a 2-dimensional, 4-segment link-segment structure to model the prosthetic leg of a unilateral amputee wearing a transfemoral prosthesis (Figure 1). The model consisted of a trunk segment, an upper leg segment (residual limb and socket), a lower leg segment (shank), and a foot segment. The connections between each segment were modeled as revolute joints. To model the foot segment, sample center of pressure (COP) data were acquired from [21, 23]. The COP data were transformed into the reference frame of the foot to compute a foot roll-over shape [21, 24].

The data for normative lower limb gait kinematics, averaged for a sample of 19 subjects, was obtained from Winter [22]. Normative gait kinematics data in literature comprise angles and positions of joints (hip, knee and ankle), position of center of pressure of the foot, and rollover shape of the foot. These data are experimentally obtained at short intervals of time through the gait cycle [22]. Using these data, and by applying inverse dynamics to the rigid body model of the prosthetic leg, the knee moment required for achieving normative joint kinematics at the hip, knee and ankle was calculated [21].

Inertial properties (mass and moment of inertia) of the upper leg, lower leg, and foot of the prosthetic leg were varied between 25% and 100% of corresponding able-bodied values, and the inverse dynamics routine was used to calculate the required knee moment for achieving normative kinematics at each joint. Upper leg mass includes the mass of the residual limb, socket, and section of the knee joint attached to the socket. The range of 25% to 100% was chosen to test configurations with inertial properties which were comparable to what a typical above-knee prosthesis user would have, and to also test values which were both higher and lower than the typical masses. The mass of the prosthetic knee joint above the axis of knee rotation was included in the mass of the upper leg. The mass below the axis of knee rotation was included in the mass of the lower leg. This information could be provided by the designer of the knee joint, or approximated by disassembling the knee joint and adding the masses of all the components above (and below) the knee axis. Approximately, a typical above-knee amputee has 50% upper leg mass and 33% lower leg and foot mass, relative to able-bodied values [20, 25]. All calculations were performed in MATLAB (R2012a, The MathWorks, Natick, MA).

Figure 2 summarizes the gross effects of inertial properties of the prosthetic leg on T_{req} [21]. Decreasing the masses of all segments of the leg relative to able-bodied values (and scaling the moments of inertia of the segments in proportion to the masses) has a large effect on T_{req} , increasing the peak magnitude during late stance by up to 43% and decreasing the peak

magnitude during swing by up to 76%. Thus, T_{req} changes significantly with the inertial properties of the prosthetic leg, indicating that MMC should be optimized to reproduce T_{req} of a prosthetic leg rather than T_{req} of an able-bodied leg. Note that moments of inertia were not varied independently from mass, as the study by Narang et al. [21] found that doing so had a negligible effect on T_{req} .

2.2 Validation and design of passive mechanical model

A mechanical model was designed to model the knee over the gait cycle. Because the aim of the present study was to determine stiffness, damping, and engagement parameters for a passive prosthetic knee, a mechanical model consisting exclusively of passive elements was considered (Figure 3). Prior to selecting components for the model, it was critical to determine whether a passive model could theoretically reproduce normative gait kinematics. To do so, knee power was computed as the product of knee moment with knee angular velocity, and net knee work was calculated as the integral of knee power with respect to time over the gait cycle. For all inertial configurations of the prosthetic leg, net knee work was negative, indicating that energy was dissipated by the knee over the gait cycle. This calculation aligned with previous studies, which found the knee to be predominantly dissipative over the gait cycle [22, 26]. Thus, a passive mechanical model of the knee can theoretically reproduce normative gait kinematics, as no net energy source is required.

2.3 Identification of phases based on knee power

Inspired by the work of Gates [27] for the ankle, the knee power versus time graph was analyzed to determine regions of gait for which specific passive mechanical elements could accurately model the knee (Figure 4). To simplify the model and subsequent optimization, only one element was selected for each region. For all inertial configurations of the prosthetic leg, the knee power versus time graph was observed to consist of three major phases: phase 1, in which the ratio of negative work (W_{neg}) to positive work (W_{pos}) is close to 1, and phases 2 and 3, in which work is purely negative. Positive work is performed when applied moment and rotation act in the same direction (such as during propulsion); negative work is performed when applied moment and rotation act in the opposite direction (such as during energy dissipation). As follows, a spring element with a clutch was selected to model the knee during phase 1, and damper elements with clutches were selected to model the knee during phase 2 and phase 3. Figure 4 illustrates the three phases for a prosthetic leg with a typical inertial configuration, with approximately 50% upper leg mass and 33% lower leg and foot mass compared to able-bodied values [20, 25].

2.4 Mathematical representation of components

In the general passive mechanical model of the knee, clutches were incorporated to engage and disengage the springs and dampers (Figure 3). To optimize MMC to reproduce T_{req} over the gait cycle, the passive mechanical components in the model were first described mathematically. The moment produced by a general, quadratic-order spring element with a clutch (T_{spr}) can be written as

$$T_{spr} = \begin{cases} -sgn(\theta - \theta_{eq})k_0 - k_1(\theta - \theta_{eq}) - sgn(\theta - \theta_{eq})k_2(\theta - \theta_{eq})^2 & t(\theta_{dis}) \leq t(\theta) \leq t(\theta_{eng}) \\ 0 & t(\theta) < t(\theta_{eng}) \quad OR \quad t(\theta) > t(\theta_{dis}), \end{cases} \quad (1)$$

where sgn is the signum function, k_0 , k_1 , and k_2 are non-negative spring coefficients, θ_{eq} is the equilibrium angle of the spring, θ_{eng} and θ_{dis} are the engagement and disengagement angles of the clutch, and the function $t(\theta)$ describes the time at which the knee angle is a given value. The signum function is used to ensure that the constant and quadratic terms produce a moment opposed to the angular displacement of the spring. Time (rather than angle) is used to describe engagement of a component because each point in time is associated with a unique angle. To allow k_0 to represent spring preload (i.e., the value of T_{spr} as soon as the clutch is engaged), the arbitrary parameter θ_{eq} is assigned to be equal to θ_{eng} . Physically, k_0 represents spring preload, k_1 represents linear spring stiffness, and k_2 represents quadratic spring stiffness.

Analogously, the moment produced by a general, second-order damper element with a clutch (T_{dmp}) can be written as

$$T_{dmp} = \begin{cases} -sgn(\dot{\theta})b_0 - b_1\dot{\theta} - sgn(\dot{\theta})b_2\dot{\theta}^2 & t(\theta_{dis}) \leq t(\theta) \leq t(\theta_{eng}) \\ 0 & t(\theta) < t(\theta_{eng}) \quad OR \quad t(\theta) > t(\theta_{dis}), \end{cases} \quad (2)$$

where b_0 , b_1 , and b_2 are non-negative damper coefficients, and the remaining parameters are the same as for the spring. Physically, b_0 represents constant friction damping, b_1 represents linear viscous damping, and b_2 represents quadratic damping.

2.5 Optimization of coefficients

MMC were optimized in each phase to minimize a cost function (C) defined as the least-squares error between the moment produced by the mechanical model (T_{mod}) and T_{req} over time. Mathematically, C was written as

$$\begin{aligned} C &= \sum_{i=1}^N (T_{req_i} - T_{mod_i})^2 \\ &= \sum_{i=1}^N (T_{req_i} - (T_{spr_1} + T_{dmp_2} + T_{dmp_3})_i)^2, \end{aligned} \quad (3)$$

where N is the number of data points in T_{req} (determined by the normative kinematic data used to compute it), T_{spr_1} is the

moment produced by the spring in phase 1, T_{dmp_2} is the moment produced by the damper in phase 2, and T_{dmp_3} is the moment produced by the damper in phase 3. Subscript $i = 1$ corresponds to heel strike, and $i = N$ corresponds to the subsequent heel strike of the ipsilateral foot. Parameter $N = 51$ for the normative kinematic data sets used in this study [22].

Optimization of MMC was performed using the *ga* (genetic algorithm) tool in the MATLAB Optimization Toolbox. Table 1 shows the lower and upper bounds prescribed for each optimized coefficient in each phase. The lower bounds for the stiffness and damping coefficients were all set to 0 to prevent selection of negative values, and upper bounds were chosen to allow a very large range of possible values, providing a large solution space for optimization.

Finally, to ensure that the model was physically realistic, the following additional constraints were applied to the optimization:

1. For the clutch in each phase, $t(\theta_{dis}) > t(\theta_{eng})$ (The clutch was required to disengage *after* it engaged.)
2. For the clutch of the spring, $\theta_{eng} = \theta_{dis}$ (All the energy stored in the spring was required to be released by the end of the phase.)

2.6 Sensitivity of cost to spring and damper complexity

A sensitivity analysis was performed in which all possible mathematical representations (i.e., all combinations of constant, linear, and quadratic terms) of each spring and damper were evaluated. For each representation, the coefficients were optimized to allow the component to best reproduce T_{req} for a prosthetic leg with a typical inertial configuration (mass of upper leg = 50% of able-bodied value, and masses of lower leg and foot = 33% of able-bodied values [20, 25]), and C was computed. Values of C were then compared to determine the simplest possible representation of each spring and damper that allowed it to accurately reproduce T_{req} during its corresponding phase.

2.7 Effects of inertial properties and cadence on optimal MMC

Using the simplest accurate representation for each spring and damper, MMC were determined for various masses of the segments of the prosthetic leg. In total, four upper leg masses (25%, 50%, 75%, and 100% of able-bodied value), seven lower leg masses (evenly distributed between 25% and 100%), and seven foot masses (evenly distributed between 25% and 100%) were investigated, comprising a total of 196 inertial configurations. In addition, the effect of walking cadence on MMC and corresponding C was calculated. Walking cadences were varied between slow (approximately 85 steps/min), natural (105 steps/min), and fast (approximately 125 steps/min) [22, 23, 28].

3 Results

3.1 Sensitivity of cost to spring and damper complexity

Table 2 shows the results of the sensitivity analysis examining the effect of the mathematical representation of components on cost. For each phase, cost was minimal for the most complex representation. However, during phase 1, cost could be reduced to within 1.0% of its minimum value by using a linear (L) spring in the mechanical model. In addition, for both phase 2 and phase 3, cost could alternatively be reduced to its minimum value by using a constant-force (K) damper.

Thus, a simple mechanical model consisting of a linear spring and two constant-force dampers (physically, a torsional spring with a linear moment-angular displacement relationship and two friction dampers) could reproduce T_{req} over the gait cycle to a nearly equivalent accuracy as the most complex model considered (coefficient of determination, $R^2 = 0.90$). Figure 5 illustrates the behavior of the simple model over the gait cycle for a prosthetic leg with a typical inertial configuration. The difference between T_{mod}^* and T_{req}^* around 45% of the gait cycle is a consequence of the negative work, W_{neg} , to positive work, W_{pos} , ratio of less than one during phase 1, meaning that more energy is generated than dissipated (Figure 4). Thus, a single passive mechanical component cannot perfectly reproduce T_{req} during this phase.

3.2 Effects of inertial properties on MMC

Figure 6 illustrates the effects of upper leg, lower leg, and foot mass on optimal MMC. The figure consists of twelve contour plots arranged in three rows and four columns. Labels m_{ul}^* , m_{ll}^* , and m_f^* designate upper leg mass, lower leg mass, and foot mass, respectively, normalized to the masses of corresponding able-bodied segments. Labels “phase 1: k_1 ”, “phase 2: b_0 ”, and “phase 3: b_0 ” designate the optimal linear stiffness coefficient during phase 1, the optimal constant damping coefficient during phase 2, and the optimal constant damping coefficient during phase 3, respectively.

To understand the plots, it is useful to consider an example. Suppose a hypothetical prosthetic leg has an upper leg (socket and residual limb) mass equal to 75% of the corresponding able-bodied value, a lower leg (shank) mass equal to 50% of the corresponding able-bodied value, and a foot mass equal to 60% of the corresponding able-bodied value ($m_{ul}^* = 75\%$, $m_{ll}^* = 50\%$, and $m_f^* = 60\%$). The optimal linear stiffness coefficient during phase 1 for this prosthetic leg can be found by looking at the graph in the first row from the top (which provides optimal linear stiffness coefficients during phase 1) and the third column from the left (which corresponds to an upper leg mass of 75%). On this graph, the optimal stiffness coefficient is found by traversing to 50% on the horizontal axis (which corresponds to 50% lower leg mass) and 60% on the vertical axis (which corresponds to 60% foot mass) and comparing the color to the color bar on the right. Here, it is seen that the stiffness coefficient is equal to approximately 2.87 [Nm/(kg*rad)]. This process can be repeated in rows 2 and 3 to find the optimal constant damping coefficient during phase 2 and the optimal constant damping coefficient during phase 3, respectively. For clarity, the points corresponding to the optimal stiffness and damping coefficients for this example prosthetic leg are encircled in black and their values pointed to by arrows on the color bars. As a whole, Figure 6 parametrically illustrates the sensitivity of MMC to varying m_{ul}^* , m_{ll}^* , and m_f^* .

The sensitivity trends are summarized as follows: optimal k_1 during phase 1 was relatively insensitive to changes in masses of prosthetic leg segments, optimal b_0 during phase 2 was moderately sensitive, and optimal b_0 during phase 3 was highly sensitive. Specifically, k_1 during phase 1, b_0 during phase 2, and b_0 during phase 3 varied by up to 5.6%, 36%, and 330%, respectively, relative to their minimum values.

For optimal k_1 during phase 1, k_1 generally increased with upper leg, lower leg, and foot mass, with some exceptions for foot mass at higher upper leg masses ($m_{ul}^* = 75\%$ and 100%). Upper leg mass had the greatest influence on k_1 . As m_{ul}^* varied between 25% and 100%, k_1 increased by up to 4.2%. However, as m_{ll}^* and m_f^* varied, k_1 increased by no more than 2.5% and 1.0%, respectively.

For optimal b_0 during phase 2, b_0 generally decreased with upper leg and lower leg mass, but varied inconsistently with foot mass. Lower leg mass had the greatest influence on b_0 . As m_{ll}^* varied between 25% and 100%, b_0 decreased by up to 27%. On the other hand, as m_{ul}^* varied, b_0 decreased by no more than 8.0%, and as m_f^* varied, b_0 changed by no more than 2.7% from its minimum to maximum values.

Finally, for optimal b_0 during phase 3, b_0 consistently increased with upper leg, lower leg, and foot mass. Foot mass had the greatest influence on b_0 , but both upper leg and foot mass had a large influence as well. Specifically, as m_f^* increased from 25% to 100%, b_0 increased by up to 180%. In comparison, as m_{ll}^* and m_{ul}^* increased, b_0 increased by up to 134% and 45%, respectively.

In summary, k_1 during phase 1 was relatively insensitive to the mass of the prosthetic leg, whereas b_0 during phase 3 was highly sensitive. Upper leg mass had the greatest influence on k_1 during phase 1, and lower leg mass had the greatest influence on b_0 during phase 2. Upper leg, lower leg, and foot mass all had a large influence on b_0 during phase 3, but foot mass had the greatest influence.

3.3 Effects of cadence on MMC

Table 3 shows the effects of walking cadence on optimal MMC for a prosthesis with a typical inertial configuration. All parameters change significantly across cadences, with b_0 during phase 3 varying the most. Specifically, k_1 during phase 1, b_0 during phase 2, and b_0 during phase 3 vary by 33%, 50%, and 100%, respectively, relative to their minimum values. In addition, cost varies by 63% relative to its minimum value. However, from an absolute perspective, cost is low ($C^* < 0.10$) at all cadences, indicating that T_{mod} consistently reproduces T_{req} .

4 Discussion

4.1 Comparison to previous work

In the present study, we designed a mechanical model using simple, passive mechanical elements and determined MMC to best reproduce T_{req} for a prosthetic leg across a wide range of inertial configurations. Because previous studies focused on determining MMC for an able-bodied leg, the only results of the present study that can be directly compared to those of previous studies are the MMC of the prosthetic leg with an able-bodied inertial configuration (i.e., upper leg, lower leg, and foot mass = 100% of able-bodied values).

For the able-bodied inertial configuration, the results closely match those of previous studies. The present study modeled the knee during phase 1 as a linear spring with a spring coefficient of $2.96 \left[\frac{N*m}{kg*rad} \right]$ (top-right of Figure 6). Shamaei & Dollar [18] modeled the knee as a linear spring with a spring coefficient of $2.92 \left[\frac{N*m}{kg*rad} \right]$ during the weight acceptance phase, which corresponds closely with phase 1. Furthermore, Sup et al. [11] modeled the knee with a linear spring, cubic spring, and linear damper and found the linear spring coefficient to be $2.89 \left[\frac{N*m}{kg*rad} \right]$ during another segment of gait corresponding with phase 1. The spring coefficient of the present study and those of Shamaei et al. and Sup et al. are nearly equivalent, differing by no more than 2.1%. On the other hand, Martinez-Villalpando and Herr [12] modeled the knee during stance as two linear springs with partially overlapped engagement and found the spring coefficient of the first spring to be $1.95 \left[\frac{N*m}{kg*rad} \right]$. The

large (34%) difference between the spring coefficient of the present study and that of Martinez-Villalpando and Herr is likely because the present study derived T_{req} based on averages across 19 subjects [22], whereas the study by Martinez-Villalpando and Herr derived T_{req} from measurement of a single subject. Recently, Shandiz et al. also designed a 7-segment model of the body, optimized joint moments to reproduce normative gait kinematics, replaced the knee with various passive controllers (e.g., springs and dampers), and optimized the controllers to preserve normative gait kinematics [29]. Although Shandiz et al. modeled the knee during stance with a linear spring, the optimized spring coefficient could not be compared to that of the present study, as the knee moments reproduced by Shandiz et al. were dramatically different from able-bodied values.

For the able-bodied inertial configuration, the present study also modeled the knee during phase 3 (approximately corresponding to swing) as a friction damper with a damping coefficient of $0.188 \frac{N \cdot m \cdot s}{kg \cdot rad}$. This result could not be compared to that of Sup et al. [11] for an analogous phase of gait, as Sup et al. modeled the knee with a linear spring, cubic spring, and viscous (rather than friction) damper.

4.2 Analysis of major findings

A simple mechanical model of the knee consisting of a first-order spring, two zero-order dampers, and three clutches accurately reproduced T_{req} for a prosthetic leg. In addition, the model was able to reproduce T_{req} nearly as accurately as a complex mechanical model consisting of nonlinear springs and dampers. Physically, this result indicates that a passive prosthetic knee with a torsional spring, constant-friction rotary dampers, and mechanical clutches may enable an above-knee amputee to walk with a very close approximation ($R^2 = 0.90$) of the knee moment required for normative kinematics.

This result has particular relevance for the development of high-performance, low-cost prostheses. Since linear springs and constant-friction dampers (e.g., friction pads) are inexpensive and mechanical clutches (e.g., contact clutches) can be easily implemented, the knee may potentially be fabricated for a low cost [30,31]. Higher order dampers such as hydraulic viscous dampers are more expensive and are also prone to leakage in adverse environmental conditions. Prosthetic knees based on this mechanical model could benefit amputees in the developing world by offering improved dynamic performance compared to existing prostheses while remaining affordable. Furthermore, such knees could also benefit amputees in the developed world by improving the passive dynamic performance of actively controlled (e.g., microprocessor-based) prostheses, potentially reducing control effort, power and moment requirements, and overall cost. Reduced power and moment requirements may also allow the use of smaller batteries, which may decrease prosthesis mass, mechanical energy expenditure, and metabolic cost at the hip [21].

The present study also found that prosthesis mass alterations, which have a large effect on T_{req} (altering peak magnitudes during stance and swing by 40-70%), cause optimal MMC to change significantly, altering coefficients by up to 180%. Although previous studies used able-bodied inertial properties to determine MMC, this result strongly suggests that designers should consider the effects of mass on MMC before selecting components for a prosthetic knee. This conclusion is supported by the study of Sup et al. [11], which found significant differences between theoretically optimized MMC and user-preferred component coefficients. The authors proposed that the inertial difference between able-bodied humans and amputees may have been the cause of this discrepancy.

Additionally, the current study computed relationships between upper leg mass, lower leg mass, foot mass, and optimal MMC in detail. The results are reported in the form of parametric illustrations that may be useful for designers of prostheses who wish to select components for a prosthetic knee. Each segment of the prosthetic leg is found to be the principal inertial determinant for a particular coefficient: the upper leg for k_1 during phase 1, the lower leg for b_0 during phase 2, and the foot for b_0 during phase 3. However, k_1 did not change significantly (no more than 5.6%) over the entire range of inertial configurations, and all three segments were found to have a large influence on b_0 during phase 3. These results suggest that alterations in prosthetic mass may not require significant adjustments in spring components used in the prosthetic knee during the weight acceptance phase, but that they may necessitate adjustment of damping components used during late stance and swing. In addition, because MMC were calculated based on knee moments normalized to body mass, component coefficients must be scaled in proportion to body mass.

Finally, the present study found that walking cadence has a significant effect on optimal MMC. From slow to fast cadences, optimal MMC varied by up to 100%. This result agrees with common knowledge that in a prosthetic knee, components need to be adjusted to the walking cadence of the user [13, 32]. To reduce the need for adjustment, future analysis should focus on identifying single components that may not perform optimally at any given cadence, but perform sufficiently well across multiple cadences.

4.3 Practical applications of the study

Prosthetists, clinicians, and designers of prosthetic knees can use the parametric illustrations in Figure 6 to tune the magnitudes of spring and damper coefficients of the prosthetic knee, based on the mass of the user and mass of the prosthesis and residual limb. For example, a unilateral transfemoral amputee who needs to be fitted with a prosthetic leg would first have the residual limb measured and weighed by the prosthetist. The masses of the rest of the prosthetic leg components (such as the socket, prosthetic knee, pylon, and prosthetic foot) can be readily measured by the prosthetist. These measurements can be used to calculate the mass of upper leg, lower leg, and foot of the prosthetic leg and normalized to the anthropometric data [23, 33–35] to determine m_{ul}^* , m_{ll}^* , and m_f^* . Figure 6 can then be used to determine the magnitudes of the optimal spring coefficient and damper coefficients required in the prosthetic knee (as discussed in section 3.2). Note that coefficient values presented in Figure 6 are normalized to body mass. The actual values of coefficients would be determined by multiplying the values on the plot by the total body mass of the user. This process could be further streamlined through development of software or a spreadsheet that performs this lookup process automatically. If the prosthetic knee is designed with modular, adjustable features, spring and damper coefficients could be easily tuned to achieve the desired magnitudes [30, 31].

4.4 Limitations of the study

Although T_{mod} was optimized to closely reproduce T_{req} , the reproduction was not exact. One resulting practical limitation is that the neuromuscular control system of the amputee may not be able to provide compensatory moments to produce normative kinematics. However, comparison of the modeled knee power with able-bodied knee power shows that only an additional 15% of the total generative knee work would be required (in order to match the able-bodied knee power). This

additional work would be required during the end of phase 1, as shown in the hatched region of Figure 5C. The knee power calculated from the mechanical model in this study was found to be within the same range of difference as that observed in above-knee amputees walking with an active knee prosthesis such as the C-leg [36]. In fact, transfemoral amputees using state-of-the-art prostheses still do not express certain normative kinematic features, such as early-stance knee flexion [25]. However, if the neuromuscular control system were not able to provide normative kinematics at any point in the gait cycle, the knee moment produced by the model would need to be modified to minimize accumulated kinematic error. Determining the extent of the modification would require forward dynamic simulation, which has well-known challenges and limitations, such as determining interaction forces between accurate mechanical models of the foot and the ground. [37,38].

In addition, since the prosthetic knee moment for normative gait kinematics was calculated by application of inverse dynamics to the model, it was assumed that the above-knee prosthesis provided the ankle moment necessary for achieving normative gait kinematics at the foot. As the net energy produced at the ankle over the gait cycle is positive for all prosthesis inertial configurations examined [22], the proposed prosthesis design could enable normative foot kinematics only if the ankle joint provided the desired power (through the gait cycle). Recently developed powered ankle-foot prostheses may be able to generate required power for normative gait kinematics [39,40]. Low-cost, powered ankles for developing countries, however, have not yet been developed. However, design optimization of passive lower limb prostheses that store and return energy during a step, to behave as close to a physiological foot as possible, is still an active area of research with encouraging results [41–44].

Another limitation of the study is the restricted range of mechanical models examined. Although our power analysis divided gait into three phases and determined the component that best replicates the energy characteristic of each phase, only one component was allowed to engage during each interval. Eliminating this constraint would lead to a significant increase in the complexity of optimization and physical implementation, but the results may justify the effort. For instance, if an additional spring were engaged during both phase 1 and phase 3, energy stored in the spring during phase 3 could supplement energy released by the original spring in phase 1, allowing the amputee to more easily initiate pre-swing flexion at 45% of the gait cycle (Figure 5).

Finally, the present study found viscous dampers (i.e., first-order dampers) to reproduce T_{req} less accurately than constant-friction dampers for walking at a natural cadence; however, viscous dampers are well-known in the prosthetics community for allowing amputees to walk comfortably at multiple cadences [32,45]. The variation of optimal constant-friction damping coefficients and optimal viscous damping coefficients across cadences and their ability to accurately reproduce T_{req} at all cadences could be compared in future.

4.5 Future work

Our ongoing work towards developing the next generation prosthetic knee for developing countries is focused on four fronts. First, we have made significant progress towards the mechanism design of a prosthetic knee that uses one spring for early stance flexion-extension and two dampers of different magnitudes for late stance flexion and swing extension [30,31]. The spring coefficient and damper coefficients used in the early prototype were selected based on the methods used in

this study [21, 46]. The prototype was tested on six subjects at the Jaipur Foot clinic (at Jaipur, India), with encouraging qualitative feedback from each of the subjects. Our future work in this direction will involve quantitative gait analysis of subjects walking with the prototype.

Second, we have conducted a detailed user-needs and stakeholder analysis to determine the exact functional requirements of amputees in India [9, 47]. Some of these functional requirements were found to be uniquely different, as compared to those in the developed world. For example, full squatting and cross legged sitting were found to be particularly important to users in India. These activities pose technical challenges that are yet to be addressed by researchers and designers of passive prosthetic knees.

Third, based on the methods presented in this study, which were focused on replicating the normative gait of level ground walking, we aim to optimize MMC for additional activities of daily living. Some of these activities, such as running, walking fast, climbing stairs, and squatting are particularly important for Indian amputees [9, 47]. A similar analysis as that presented in this study of normative gait patterns of these activities can lead to the design of a multipurpose knee, which has been optimized for multiple activities.

Fourth, further work is needed towards refinement and validation of the methods, analysis and results presented in this study and previous work by Narang et al. [21]. Forward dynamics simulations may help determine if the knee moment and the mechanical model implemented in our present study will result in normative gait kinematics for a transfemoral amputee. Future studies can also focus on comparing the performance of constant-friction and viscous dampers across multiple cadences, as well as reducing restrictions on the engagement of components in the model to more accurately reproduce the knee moment required for normative kinematics.

5 Conclusion

The present study aimed to determine the optimal stiffness, damping, and engagement parameters for a low-cost, passive prosthetic knee through the design and optimization of a mechanical model. Inverse dynamics was used to determine the knee moment required for a prosthetic leg to walk with normative kinematics. A simple mechanical model of the knee was designed and optimized to accurately replicate the required knee moment. Mass of the prosthetic leg was found to have a significant effect on the required knee moment, and upper leg mass, lower leg mass, and foot mass were each found to have a significant influence on the optimal coefficients of the components in the model, particularly the damping coefficients.

In contrast to previous studies, the present study used power analysis of the knee to select components for the mechanical model, used sensitivity analysis to identify the simplest mathematical representation of each component, and optimized the coefficients of each component to reproduce the moment required for a typically lightweight prosthetic leg (rather than an able-bodied leg) to walk with normative kinematics. In addition, the study computed the effects of the mass of each segment of the prosthetic leg on optimal coefficients and reported the results in a parametric illustration that can be used by designers and prosthetists. Future work should focus on comparing the results of this study with those obtained by experimental gait analysis of knee prototypes designed using the results presented here, and forward dynamics simulations. Optimization of mechanical component coefficients for multiple activities of daily living could facilitate the design of a multipurpose knee,

which can be widely adopted in India.

6 Acknowledgments

We would like to acknowledge Dr. Pooja Mukul and the rest of the staff at Bhagwan Mahaveer Viklang Sahayata Samiti (BMVSS, a.k.a., the Jaipur Foot organization, Jaipur, India) for their partnership in our work. Funding for this study was provided by the Pappalardo Mechanical Engineering Research Fellowship at the Massachusetts Institute of Technology (MIT), the MIT Public Service Center, the MIT Research Support Committee, the National Science Foundation Graduate Research Fellowship under Grant No. 1122374, and the Tata Center for Technology and Design at MIT.

References

- [1] World Health Organization, 2005. Guidelines for Training Personnel in Developing Countries for Prosthetics and Orthotics Services. Tech. rep., World Health Organization.
- [2] World Health Organization, 2011. World Report on Disability. Tech. rep., World Health Organization.
- [3] Hamner, S. R., Narayan, V. G., and Donaldson, K. M., 2013. “Designing for Scale: Development of the ReMotion Knee for Global Emerging Markets.”. *Annals of Biomedical Engineering*, **41**(9), Sept., pp. 1851–9.
- [4] Narang, I., and Jape, V., 1982. “Retrospective study of 14,400 civilian disabled treated over 25 years at an Artificial Limb Center”. *Prosthetics and Orthotics International*, **6**, pp. 10–16.
- [5] Central Intelligence Agency, 2013. The CIA World Factbook 2014. Tech. rep., Central Intelligence Agency, Washington, D.C.
- [6] Mohan, D., 1967. “A Report on Amputees in India”. *Orthotics and Prosthetics*, **40**(1), pp. 16–32.
- [7] Jensen, J. S., and Raab, W., 2004. “Clinical field testing of transfemoral prosthetic technologies: resin-wood and ICRC-polypropylene”. *Prosthetics and Orthotics International*, **28**(2), pp. 141–151.
- [8] Bhagwan Mahaveer Viklang Sahayata Samiti, 2014. What We Do: Above Knee Prosthesis. http://jaipurfoot.org/what_we_do/prosthesis/above_knee_prosthesis.html (Accessed 5/19/14).
- [9] Narang, Y. S., 2013. “Identification of Design Requirements for a High-Performance , Low-Cost , Passive Prosthetic Knee Through User Analysis and Dynamic Simulation by”. Master’s thesis, Massachusetts Institute of Technology, Cambridge MA, May.
- [10] Kuo, A. D., and Donelan, J. M., 2010. “Dynamic principles of gait and their clinical implications”. *Physical Therapy*, **90**(2), pp. 157–74.
- [11] Sup, F., Bohara, A., and Goldfarb, M., 2008. “Design and control of a powered transfemoral prosthesis”. *The International Journal of Robotics Research*, **27**(2), pp. 263–73.
- [12] Martinez-Villalpando, E. C., and Herr, H., 2009. “Agonist-antagonist active knee prosthesis: A preliminary study in level-ground walking”. *Journal of Rehabilitation Research & Development*, **46**(3), pp. 361–74.
- [13] Berry, D., 2006. “Microprocessor prosthetic knees”. *Physical Medicine and Rehabilitation Clinics of North America*, **17**, pp. 91–113.

- [14] Smith, D. G., Michael, J. W., and Bowker, J. H., 2004. *Atlas of amputations and limb deficiencies: surgical, prosthetic, and rehabilitation principles*, Vol. 3. American Academy of Orthopaedic Surgeons Rosemont, IL.
- [15] Andrysek, J., 2010. “Lower-limb prosthetic technologies in the developing world: a review of literature from 1994–2010”. *Prosthetics and orthotics international*, **34**(4), pp. 378–398.
- [16] Andrysek, J., Klejman, S., Torres-Moreno, R., Heim, W., Steinnagel, B., and Glasford, S., 2011. “Mobility function of a prosthetic knee joint with an automatic stance phase lock”. *Prosthetics and Orthotics International*, **35**(2), pp. 163–70.
- [17] Frigo, C., Crenna, P., and Jensen, L., 1996. “Moment-angle relationship at lower limb joints during human walking at different velocities”. *Journal of Electromyography and Kinesiology*, **6**(3), pp. 177–90.
- [18] Shamaei, K., and Dollar, A. M., 2011. “On the mechanics of the knee during the stance phase of the gait”. In 2011 IEEE International Conference on Rehabilitation Robotics.
- [19] Shamaei, K., Sawicki, G. S., and Dollar, A. M., 2013. “Estimation of quasi-stiffness of the human knee in the stance phase of walking”. *PLoS ONE*, **8**(3), p. e59993.
- [20] Czerniecki, J. M., Gitter, A., and Weaver, K., 1994. “Effect of alterations in prosthetic shank mass on the metabolic costs of ambulation in above-knee amputees”. *American Journal of Physical Medicine & Rehabilitation*, **73**, pp. 348–352.
- [21] Narang, Y., Arelekatti, V. N. M., and Winter, A., 2015. “The effects of prosthesis inertial properties on prosthetic knee moment and hip energetics required to achieve able-bodied kinematics”. *Neural Systems and Rehabilitation Engineering, IEEE Transactions on*, **In Press**(DOI: 10.1109/TNSRE.2015.2455054).
- [22] Winter, D. A., 1991. *The Biomechanics and Motor Control of Human Gait: Normal, Elderly, and Pathological*, 2nd ed. Waterloo Biomechanics.
- [23] Winter, D. A., 2009. *Biomechanics and Motor Control of Human Movement*, 4th ed. John Wiley & Sons, Inc.
- [24] Hansen, A. H., Childress, D. S., and Knox, E. H., 2004. “Roll-over shapes of human locomotor systems: effects of walking speed”. *Clinical Biomechanics*, **19**, pp. 407–14.
- [25] Johansson, J. L., Sherrill, D. M., Riley, P. O., Bonato, P., and Herr, H., 2005. “A clinical comparison of variable-damping and mechanically passive prosthetic knee devices”. *American Journal of Physical Medicine & Rehabilitation*, **84**(8), pp. 563–75.
- [26] Winter, D. A., 1983. “Energy generation and absorption at the ankle and knee during fast, natural, and slow cadences.”. *Clinical orthopaedics and related research*(175), May, pp. 147–54.
- [27] Gates, D. H., 2004. “Characterizing ankle function during stair ascent, descent, and level walking for ankle prosthesis and orthosis design”. Master’s thesis, Massachusetts Institute of Technology.
- [28] Winter, D. A., 1983. “Biomechanical motor patterns in normal walking”. *Journal of Motor Behavior*, **15**(4), pp. 302–30.
- [29] Shandiz, M. A., Farahmand, F., Osman, N. A. A., and Zohoor, H., 2013. “A Robotic Model of Transfemoral Amputee Locomotion for Design Optimization of Knee Controllers”. *International Journal of Advanced Robotic Systems*, p. 1.
- [30] Arelekatti, V. N. M., and Winter, A. G., 2015. “Design of a fully passive prosthetic knee mechanism for transfemoral amputees in india”. In IEEE International Conference on Rehabilitation Robotics (ICORR), 2015, IEEE. Accepted.

- [31] Arelekatti, V. N. M., and Winter, A. G., 2015. "Design of mechanism and preliminary field validation of low-cost, passive prosthetic knee for users with transfemoral amputation in india". In ASME 2015 International Design Engineering Technical Conferences and Computers and Information in Engineering Conference, American Society of Mechanical Engineers. Accepted.
- [32] Michael, J., 1999. "Modern prosthetic knee mechanisms". *Clinical Orthopaedics and Related Research*(361), pp. 39–47.
- [33] Drillis, R., and Contini, R., 1966. Body segment parameters. Tech. rep., Office of Vocational Rehabilitation, Department of Health, Education, and Welfare, New York.
- [34] Miller, D. I., and Nelson, R. C., 1973. *The Biomechanics of Sport: A Research Approach*. Lea & Febiger, Philadelphia.
- [35] Plagenhoef, S., 1971. *Patterns of Human Motion: A Cinematographic Analysis*. Prentice Hall.
- [36] Segal, A. D., Orendurff, M. S., Klute, G. K., McDowell, M. L., Pecoraro, J. a., Shofer, J., and Czerniecki, J. M., 2006. "Kinematic and kinetic comparisons of transfemoral amputee gait using C-Leg and Mauch SNS prosthetic knees". *The Journal of Rehabilitation Research and Development*, **43**(7), p. 857.
- [37] Pandy, M. G., 2001. "Computer modeling and simulation of human movement". *Annual Review of Biomedical Engineering*, **3**, pp. 245–73.
- [38] Meglan, D. A., 1991. "Enhanced analysis of human locomotion". PhD thesis, The Ohio State University.
- [39] Au, S., Berniker, M., and Herr, H., 2008. "Powered ankle-foot prosthesis to assist level-ground and stair-descent gaits". *Neural Networks*, **21**, pp. 654–66.
- [40] BiOM, 2014. Biom T2 system. <http://www.biom.com/patients/biom-t2-system/> (Accessed 05/19/14).
- [41] Hafner, B. J., 2005. "Clinical prescription and use of prosthetic foot and ankle mechanisms: a review of the literature". *JPO: Journal of Prosthetics and Orthotics*, **17**(4), pp. S5–S11.
- [42] Hafner, B. J., Sanders, J. E., Czerniecki, J. M., and Ferguson, J., 2002. "Transtibial energy-storage-and-return prosthetic devices: a review of energy concepts and a proposed nomenclature". *Journal of rehabilitation research and development*, **39**(1), pp. 1–12.
- [43] Hafner, B. J., Sanders, J. E., Czerniecki, J., and Ferguson, J., 2002. "Energy storage and return prostheses: does patient perception correlate with biomechanical analysis?". *Clinical Biomechanics*, **17**(5), pp. 325–344.
- [44] Unal, R., Klijnstra, F., Burkink, B., Behrens, S., Hekman, E., Stramigioli, S., Koopman, H., and Carloni, R., 2013. "Modeling of walkmech: a fully-passive energy-efficient transfemoral prosthesis prototype". In Rehabilitation Robotics (ICORR), 2013 IEEE International Conference on, IEEE, pp. 1–6.
- [45] Romo, H. D., 2000. "Prosthetic knees". *New Developments in Prosthetics and Orthotics*, **11**(3).
- [46] Narang, Y. S., and Winter, A. G., 2014. "Effects of prosthesis mass on hip energetics, prosthetic knee torque, and prosthetic knee stiffness and damping parameters required for transfemoral amputees to walk with normative kinematics". In ASME 2014 International Design Engineering Technical Conferences and Computers and Information in Engineering Conference, American Society of Mechanical Engineers, pp. V05AT08A017–V05AT08A017.

[47] Narang, Y., , Austin-Breneman, J., Arelekatti, V. N. M., and Winter, A., 2015. “Using biomechanical and human-centered analysis to determine design requirements for a prosthetic knee for use in india”. *In review*.

List of Tables

1 Lower and upper bounds for all the coefficients optimized in each phase (Figure 4). All coefficients are normalized to body mass. Symbols t_{i1} and t_{f1} designate the initial time and final time in phase 1, t_{i2} and t_{f2} designate the initial time and final time in phase 2, and t_{i3} and t_{f3} designate the initial time and final time in phase 3. 21

2 Sensitivity of optimization cost to the complexity of components. Cost is reported as C^* , which is equal to C normalized to the maximum theoretical cost during the corresponding phase (i.e., the cost during that phase when no components are used to model the knee). For a given component, K designates a mathematical representation with just a constant term, L just a linear term, and Q just a quadratic term. Combinations of K, L, and Q designate mathematical representations in which more than one term are included. (For example, KL for a damper indicates a mathematical representation of $M_{dmp} = -sgn(\dot{\theta})b_0 - b_1\dot{\theta}$) 22

3 The effects of walking cadence on optimal MMC and corresponding cost for a prosthesis with a typical inertial configuration (upper leg mass = 50% of able-bodied value, and lower leg and foot mass = 33% of able-bodied values). C^* is equal to C normalized to the maximum theoretical cost over the gait cycle (i.e., the cost over the gait cycle when no components are used to model the knee). 23

List of Figures

- 1 2-dimensional, 4-segment link structure to model the prosthetic leg of a unilateral amputee wearing a trans-femoral prosthesis. The model consisted of a trunk segment, an upper leg segment (residual limb and socket), a lower leg segment (shank), and a foot segment. The connections between each segment were modeled as revolute joints. 24
- 2 Gross effects of altering inertial properties on the knee moment required for a prosthetic leg to move with normative kinematics. Symbol T_{req}^* designates the required knee moment normalized to body mass. The masses of all segments of the leg are scaled to the specified percentages of able-bodied values, and the moments of inertia (about the centers of mass of the segments) are scaled in proportion. 25
- 3 Schematic of general passive mechanical model used to model the knee. Symbol θ designates the knee joint angle. 26
- 4 Three energy-based phases of gait. Normalized knee power versus time graph (solid blue curve) is shown for a prosthetic leg with a typical inertial configuration (upper leg mass = 50% of able-bodied value, and lower leg and foot mass = 33% of able-bodied values [20, 25]) moving with normative kinematics. Symbol P_k^* designates knee power normalized to body mass. Phase 1 is a negative and positive work phase ($\frac{W_{neg}}{W_{pos}} = 0.77$), which can be partially replicated with a spring element, and phases 2 and 3 are purely negative work phases ($W_{pos} = 0$), which can be accurately replicated with dampers. Normalized knee power versus time graph (dashed red curve) is also shown for able-bodied values of segment masses [22] (upper leg mass = 100% of able-bodied value, and lower leg and foot mass = 100% of able-bodied values). 27
- 5 Behavior of simplified mechanical model over the gait cycle. The model was optimized to reproduce knee moment, T_{req} , of a prosthetic leg with a typical inertial configuration (mass of upper leg = 50% of able-bodied value, and masses of lower leg and foot = 33% of able-bodied values). (A) Illustration of optimized engagement (θ_{eng}) and disengagement (θ_{dis}) angles of the clutch for each component. (B) Comparison of knee moment normalized to body mass for normative kinematics (T_{req}^*) and produced by the mechanical model (T_{mod}^*). Agreement between T_{req}^* and T_{mod}^* is $R^2 = 0.90$. Labels k_1 and b_0 designate the linear spring coefficient and constant damping coefficient for a given phase. Note that the difference between T_{mod}^* and T_{req}^* around 45% of the gait cycle is a consequence of a negative work, W_{neg} , to positive work, W_{pos} , ratio of less than one during phase 1, meaning that more energy is generated than dissipated (Figure 4). Thus, a single passive mechanical component cannot perfectly reproduce T_{req} during phase 1. (C) Comparison of knee power (normalized to body mass) required for normative kinematics and knee power produced by the mechanical model. Knee power is calculated as the product of knee moment (modeled or required) and able-bodied angular velocity of the knee joint. Agreement between required knee power and modeled knee power is $R^2 = 0.91$. Hatched areas show where the modeled knee power is insufficient and is less than the generative knee power required for normative gait kinematics. 28

6 Parametric illustrations showing the effects of leg segment masses on optimal MMC. Labels m_{ul}^* , m_{ll}^* , and m_f^* designate upper leg mass, lower leg mass, and foot mass normalized to the masses of corresponding able-bodied segments. Labels “phase 1: k_1 ”, “phase 2: b_0 ”, and “phase 3: b_0 ” designate the linear stiffness coefficient during phase 1, the constant damping coefficient during phase 2, and the constant damping coefficient during phase 3, respectively, all normalized to body mass. Section 3.2 explains the method to determine MMC in this figure. Dashed lines and arrows correspond to an example leg and optimum MMC with 75% upper leg, 50% lower leg, and 60% foot masses compared to able-bodied values. 29

		Coefficient				
Phase 1 (Spring)		$k_0 [\frac{N*m}{kg}]$	$k_1 [\frac{N*m}{kg*rad}]$	$k_2 [\frac{N*m}{kg*rad^2}]$	$t(\theta_{eng}) [s]$	$t(\theta_{dis}) [s]$
	lower bound	0	0	0	t_{i1}	t_{f1}
	upper bound	5	30	200	t_{i1}	t_{f1}
Phase 2 (Damper 1)		$b_0 [\frac{N*m}{kg}]$	$b_1 [\frac{N*m*s}{kg*rad}]$	$b_2 [\frac{N*m*s^2}{kg*rad}]$	$t(\theta_{eng}) [s]$	$t(\theta_{dis}) [s]$
	lower bound	0	0	0	t_{i2}	t_{f2}
	upper bound	3	0.7	0.2	t_{i2}	t_{f2}
Phase 3 (Damper 2)		$b_0 [\frac{N*m}{kg}]$	$b_1 [\frac{N*m*s}{kg*rad}]$	$b_2 [\frac{N*m*s^2}{kg*rad}]$	$t(\theta_{eng}) [s]$	$t(\theta_{dis}) [s]$
	lower bound	0	0	0	t_{i3}	t_{f3}
	upper bound	0.7	0.1	0.02	t_{i3}	t_{f3}

Table 1. Lower and upper bounds for all the coefficients optimized in each phase (Figure 4). All coefficients are normalized to body mass. Symbols t_{i1} and t_{f1} designate the initial time and final time in phase 1, t_{i2} and t_{f2} designate the initial time and final time in phase 2, and t_{i3} and t_{f3} designate the initial time and final time in phase 3.

	C^* for each polynomial representation						
	K	L	Q	KL	LQ	KQ	KLQ
Phase 1 (Spring)	0.21	0.08	0.09	0.08	0.07	0.07	0.07
Phase 2 (Damper)	0.09	0.11	0.18	0.09	0.11	0.09	0.09
Phase 3 (Damper)	0.13	0.37	0.46	0.13	0.37	0.13	0.13

Table 2. Sensitivity of optimization cost to the complexity of components. Cost is reported as C^* , which is equal to C normalized to the maximum theoretical cost during the corresponding phase (i.e., the cost during that phase when no components are used to model the knee). For a given component, K designates a mathematical representation with just a constant term, L just a linear term, and Q just a quadratic term. Combinations of K, L, and Q designate mathematical representations in which more than one term are included. (For example, KL for a damper indicates a mathematical representation of $M_{dmp} = -sgn(\dot{\theta})b_0 - b_1\dot{\theta}$)

		Cadence		
	Parameter	Slow	Natural	Fast
Phase 1 (Spring)	$k_1 [\frac{N*m}{kg*rad}]$	3.79	2.86	3.24
Phase 2 (Damper)	$b_0 [\frac{N*m}{kg}]$	0.28	0.29	0.42
Phase 3 (Damper)	$b_0 [\frac{N*m}{kg}]$	0.039	0.069	0.078
	C^*	0.093	0.085	0.057

Table 3. The effects of walking cadence on optimal MMC and corresponding cost for a prosthesis with a typical inertial configuration (upper leg mass = 50% of able-bodied value, and lower leg and foot mass = 33% of able-bodied values). C^* is equal to C normalized to the maximum theoretical cost over the gait cycle (i.e., the cost over the gait cycle when no components are used to model the knee).

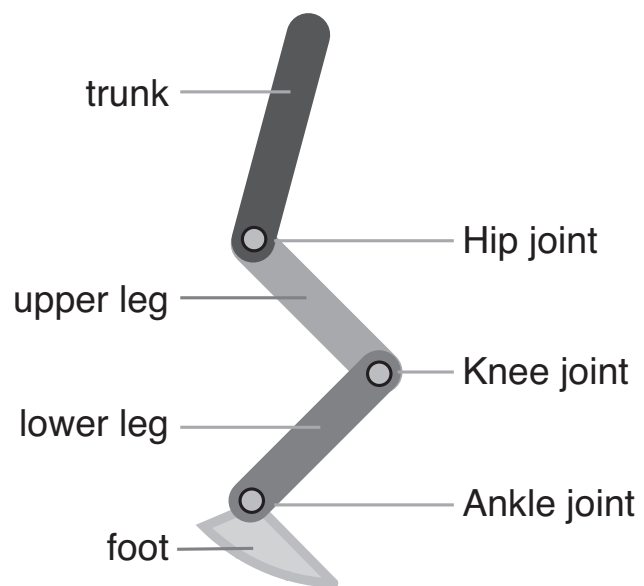


Fig. 1. 2-dimensional, 4-segment link structure to model the prosthetic leg of a unilateral amputee wearing a transfemoral prosthesis. The model consisted of a trunk segment, an upper leg segment (residual limb and socket), a lower leg segment (shank), and a foot segment. The connections between each segment were modeled as revolute joints.

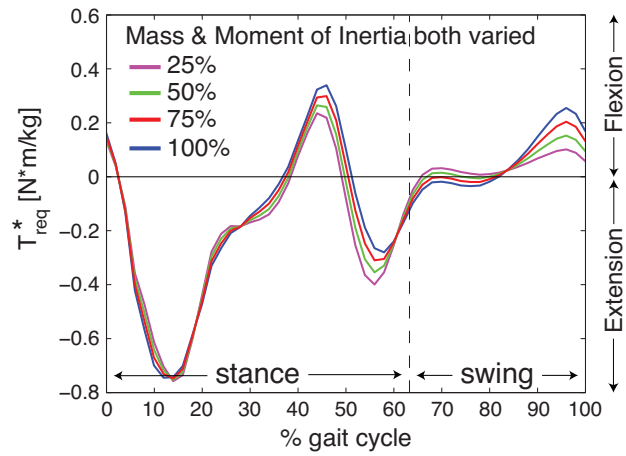


Fig. 2. Gross effects of altering inertial properties on the knee moment required for a prosthetic leg to move with normative kinematics. Symbol T_{req}^* designates the required knee moment normalized to body mass. The masses of all segments of the leg are scaled to the specified percentages of able-bodied values, and the moments of inertia (about the centers of mass of the segments) are scaled in proportion.

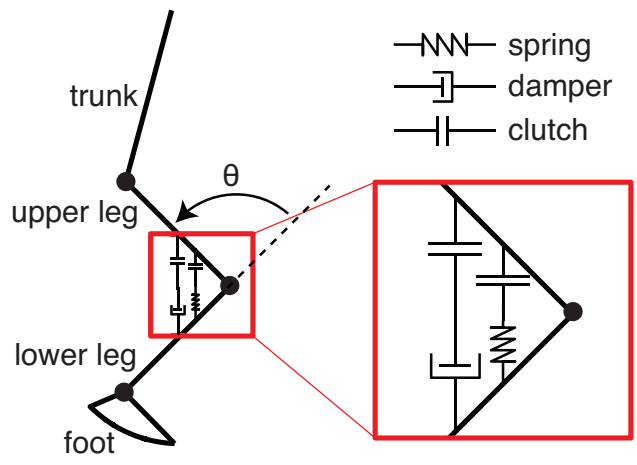


Fig. 3. Schematic of general passive mechanical model used to model the knee. Symbol θ designates the knee joint angle.

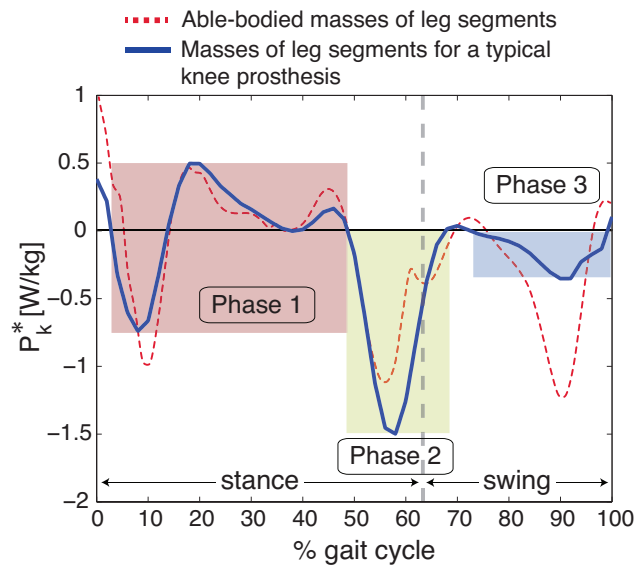


Fig. 4. Three energy-based phases of gait. Normalized knee power versus time graph (solid blue curve) is shown for a prosthetic leg with a typical inertial configuration (upper leg mass = 50% of able-bodied value, and lower leg and foot mass = 33% of able-bodied values [20, 25]) moving with normative kinematics. Symbol P_k^* designates knee power normalized to body mass. Phase 1 is a negative and positive work phase ($\frac{W_{neg}}{W_{pos}} = 0.77$), which can be partially replicated with a spring element, and phases 2 and 3 are purely negative work phases ($W_{pos} = 0$), which can be accurately replicated with dampers. Normalized knee power versus time graph (dashed red curve) is also shown for able-bodied values of segment masses [22] (upper leg mass = 100% of able-bodied value, and lower leg and foot mass = 100% of able-bodied values).

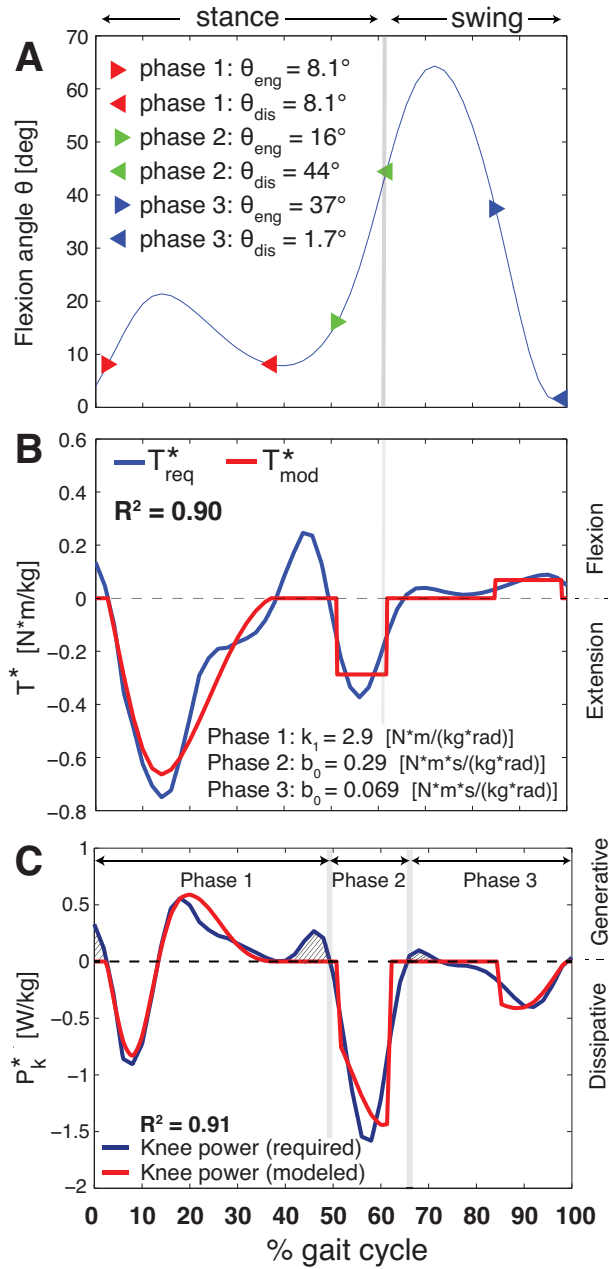


Fig. 5. Behavior of simplified mechanical model over the gait cycle. The model was optimized to reproduce knee moment, T_{req} , of a prosthetic leg with a typical inertial configuration (mass of upper leg = 50% of able-bodied value, and masses of lower leg and foot = 33% of able-bodied values). (A) Illustration of optimized engagement (θ_{eng}) and disengagement (θ_{dis}) angles of the clutch for each component. (B) Comparison of knee moment normalized to body mass for normative kinematics (T_{req}^*) and produced by the mechanical model (T_{mod}^*). Agreement between T_{req}^* and T_{mod}^* is $R^2 = 0.90$. Labels k_1 and b_0 designate the linear spring coefficient and constant damping coefficient for a given phase. Note that the difference between T_{mod}^* and T_{req}^* around 45% of the gait cycle is a consequence of a negative work, W_{neg} , to positive work, W_{pos} , ratio of less than one during phase 1, meaning that more energy is generated than dissipated (Figure 4). Thus, a single passive mechanical component cannot perfectly reproduce T_{req} during phase 1. (C) Comparison of knee power (normalized to body mass) required for normative kinematics and knee power produced by the mechanical model. Knee power is calculated as the product of knee moment (modeled or required) and able-bodied angular velocity of the knee joint. Agreement between required knee power and modeled knee power is $R^2 = 0.91$. Hatched areas show where the modeled knee power is insufficient and is less than the generative knee power required for normative gait kinematics.

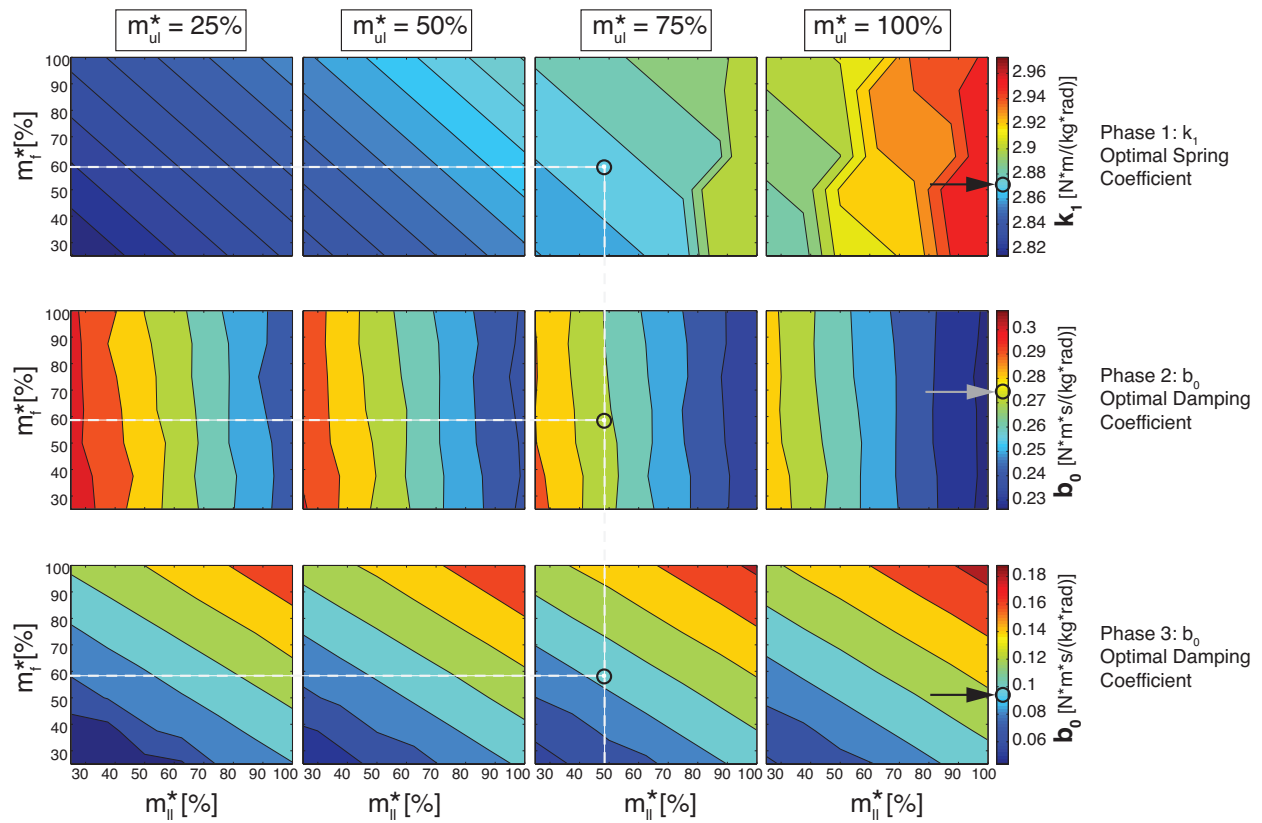


Fig. 6. Parametric illustrations showing the effects of leg segment masses on optimal MMC. Labels m_{ul}^* , m_{ll}^* , and m_f^* designate upper leg mass, lower leg mass, and foot mass normalized to the masses of corresponding able-bodied segments. Labels “phase 1: k_1 ”, “phase 2: b_0 ”, and “phase 3: b_0 ” designate the linear stiffness coefficient during phase 1, the constant damping coefficient during phase 2, and the constant damping coefficient during phase 3, respectively, all normalized to body mass. Section 3.2 explains the method to determine MMC in this figure. Dashed lines and arrows correspond to an example leg and optimum MMC with 75% upper leg, 50% lower leg, and 60% foot masses compared to able-bodied values.